

# THERMAL EFFECTS OF OVENIZED CLOCKS ON EPISEAL ENCAPSULATED INERTIAL MEASUREMENT UNITS

Lizmarie Comenencia Ortiz<sup>1</sup>, Ian B. Flader<sup>1</sup>, Gabrielle D. Vukasin<sup>1</sup>, Dustin D. Gerrard<sup>1</sup>, Saurabh A. Chandorkar<sup>1</sup>, Janna Rodriguez<sup>1</sup>, Dongsuk D. Shin<sup>1</sup>, Ryan Kwon<sup>1</sup>, David B. Heinz<sup>1</sup>, Yunhan Chen<sup>2</sup>, Woosung Park<sup>1</sup>, Kenneth E. Goodson<sup>1</sup>, and Thomas W. Kenny<sup>1</sup>

<sup>1</sup>Stanford University, Stanford, USA, <sup>2</sup>Apple Inc., Cupertino, USA

## ABSTRACT

In this paper, we demonstrate the thermal effects of micro-ovenized clocks embedded in the device layer of a vacuum sealed MEMS inertial measurement unit. We demonstrate a novel in-plane suspension and heater that provides improved thermal isolation within a mm-scale chip, compared to in-cap heaters. We show the interaction of three resonators within a single die: an ovenized tuning fork, a resonant accelerometer, and a disk resonating gyroscope. We demonstrate that a device layer micro-oven, which operates at a tenth of the power of an encapsulation cap-layer micro-oven, has very small effects on the frequency of the other resonators in the die, thus proving good thermal isolation in our structures. We show that the in-plane heater isolation provides more than a 15X reduction of frequency deviation of adjacent sensors.

## INTRODUCTION

MEMS timing references are improving in stability and precision and replacing quartz clocks. To achieve the high frequency stability required for inertial sensors, temperature compensation methods are essential. Previous work has shown that a combination of passive and active compensation methods for epitaxially encapsulated MEMS can significantly increase the stability of clocks [1-4]. Active compensation has been achieved previously with the use of a micro-oven embedded in the encapsulation lid of the structures [1, 18]; while this method is successful in compensating for temperature changes, it requires a great amount of power (approximately  $3\text{mW}/^\circ\text{C}$ ) [1]. The dissipated heat can affect the stability and performance of other sensors within the encapsulated area due to temperature gradients and thermal stresses. Therefore, it is important to minimize the dissipated heat to reduce the thermal effects in adjacent elements within the die and increase the micro-oven efficiency.

Previous work has shown that having a micro-oven within the device layer of the die can significantly reduce the power required to ovenize devices [2, 5], but no studies have shown how this method affects adjacent devices within the die. These effects are particularly important in inertial measurement units, where multiple sensors are packaged in the same die.

We demonstrate the thermal effects of a serpentine micro-oven located at the anchor of a double-ended tuning fork (DETF) in the plane of the device layer, which requires much less power (approximately  $0.3\text{mW}/^\circ\text{C}$ ). Frequency changes of a resonant accelerometer and disk resonating gyroscope (DRG) were tracked with the application of heating voltages to the ovenized DETF.

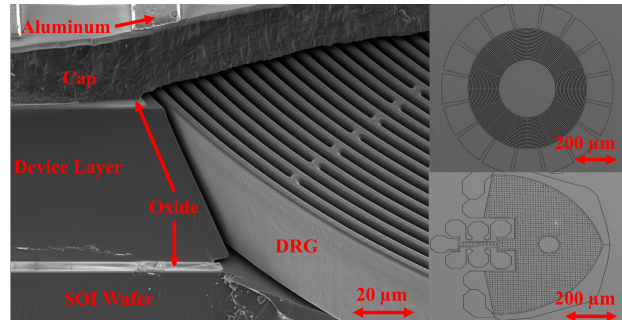


Figure 1: SEM images of episeal encapsulated disk resonating gyroscope (left and top right) and resonant accelerometer (bottom right).

We compare these results with frequency changes in a resonant accelerometer and a DRG packaged in a similar die with the application of heating voltages to an in-cap micro-oven.

## DESIGN AND FABRICATION

In this paper, we study the thermal effects of an ovenized element on adjacent sensors. We study a die with the layout described in figure 2, which contains a disk resonating gyroscope, a resonant accelerometer and an ovenized DETF. The disk resonating gyroscope has a resonant body with a radius of  $300\ \mu\text{m}$ , 16 electrodes on the sides and is anchored in the center. The resonant accelerometer, whose design is detailed in [17], has two resonating beams with dimensions of  $160\ \mu\text{m} \times 3\ \mu\text{m}$  connected to a proof mass. The ovenized DETF contains two resonating beams with dimensions of  $200\ \mu\text{m} \times 6\ \mu\text{m}$  and a micro-oven with  $7.5\ \mu\text{m}$  thick beams, located at the anchor.

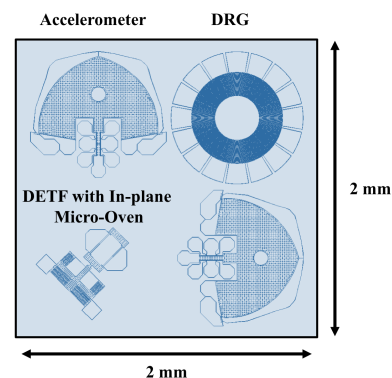


Figure 2: 2D rendering of device layer on the episeal encapsulated die.

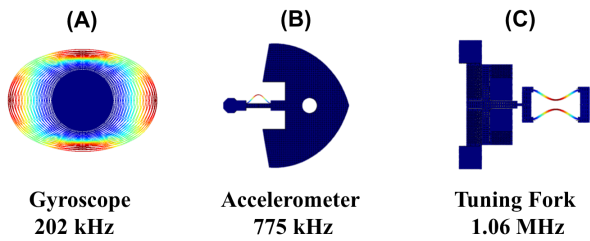


Figure 3: COMSOL simulation of eigen frequency modes for each device.

We model the eigen frequency modes for the devices, shown in figure 3. The DRG is operated with the wineglass mode (202 kHz), the accelerometer beam and the DETF beams are operated at the first order eigen frequency mode (775 kHz and 1.06 MHz respectively). The devices were fabricated in a 60  $\mu\text{m}$  device layer with a highly-doped p-type SOI aligned with the  $\langle 100 \rangle$  crystal orientation using an epitaxial vacuum encapsulation process. Figure 1 shows a cross section SEM image of the disk resonating gyroscope and SEM images of the top view of the DRG and accelerometer.

For comparison, we studied another MEMS inertial measurement unit with a similar layout and fabrication and an encapsulation layer micro-oven. In this die, the ovenized element is a 300  $\mu\text{m}$  x 300  $\mu\text{m}$  Lamé resonator with a 300  $\mu\text{m}$  x 6  $\mu\text{m}$  micro-oven located in the cap and connected at the anchor, the same design is described in [1].

## METHODS

The temperature dependence of frequency and quality factor for each resonator was determined over a range of temperatures from  $-10^\circ\text{C}$  to  $70^\circ\text{C}$ , using open loop frequency sweeps with a Zurich Instruments digital lock-in amplifier and transimpedance amplifiers to amplify the resonators' signal as shown in figure 5.

The DRG was resonated with a bias voltage of 15V and a driving AC voltage of 50mV, whereas the accelerometer was biased at 10V and was resonated with a driving AC voltage of 20mV. Two power supplies were used to apply a split-heater voltage and bias voltage of 20V to the tuning fork. A driving AC voltage of 50mV was applied at the tuning fork. The current and voltage at the micro-oven electrodes were tracked with a multimeter to ensure that the voltage applied at the heater was constant throughout the experiments.

Table 1: Comparison of encapsulation-layer and inplane micro-oven performance and thermal effects on adjacent sensors with ovenized element at  $70^\circ\text{C}$ .

		Inplane Micro-Oven	Encapsulation Micro-Oven
<b>Oven Power</b>		15 mW	$\sim 160$ mW
$\Delta f$	DRG	18.25 ppm	541 ppm
	Accel	47.22 ppm	198.8 ppm
$\Delta T$	DRG	$0.9^\circ\text{C}$	$26.9^\circ\text{C}$
	Accel	$2.5^\circ\text{C}$	$10.3^\circ\text{C}$

Infrared radiation (IR) images of the dies were obtained using a Quantum Focus InfraScope II. The images, shown in figure 5, were captured while in-plane and in-cap micro-oven devices were heated to assess how the adjacent devices within the die were affected by the temperature change in the heated elements. Approximate temperature of the ovenized element was calculated based on the micro-oven power to frequency shift ratio [4].

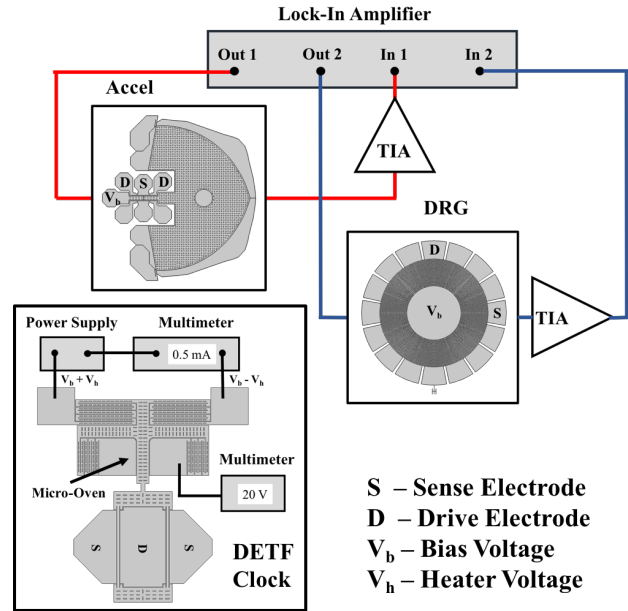


Figure 4: Experimental set up: a phase lock amplifier was used to collect open loop sweeps of two devices at a time.

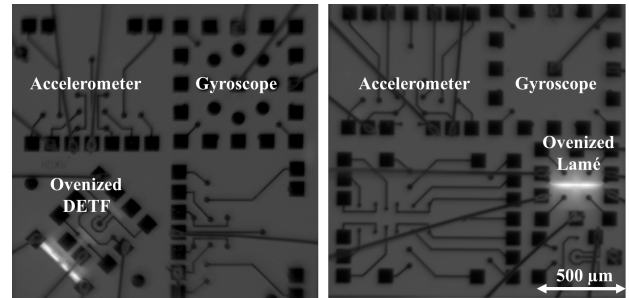


Figure 5: IR image of ovenized DETF while heating to a power of 71 mW (left), IR image of ovenized Lamé resonator while heating to a power of 159.2 mW (right).

## RESULTS

### Open Loop Frequency Sweeps

The results, shown in figure 6, demonstrate that the frequency and the quality factor of the resonating elements decreases with temperature as expected for the p-type wafer doping [3]. The open loop frequency sweeps captured at a range of temperatures, from the set up shown in figure 5, were used to map applied heating voltages at the micro-oven to the temperature at the ovenized DETF and the adjacent devices.

### Micro-oven Power and Thermal Effects

Both in-plane and in-cap ovenized devices were heated from 25°C to a device temperature of approximately 70°C. The ratio of the device temperature to micro-oven power ratio was mapped using the TCF obtained previously for the ovenized DETF and with the results discussed in [1] for a similar ovenized Lamé. As expected, the power required to achieve a temperature change of 45 °C of for the in-plane micro-oven was 15mW, whereas for the in-cap heater it was approximately 160mW.

The application of 15 mW to the DETF in-plane micro-oven caused a frequency shift for the nearby accelerometer and gyroscope of less than 50 ppm, whereas that of the ovenized tuning fork was 1000 ppm (see figure 7). Similar device temperatures in encapsulation layer micro-oven devices required approximately 160 mW heating power, documented in [1], which induced nearly 600 ppm frequency deviation in adjacent inertial sensors.

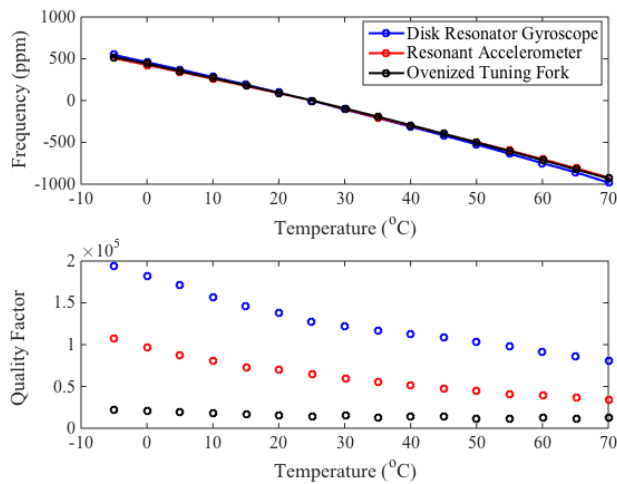


Figure 6: Frequency and quality factor with temperature captured in open loop sweeps.

Overall, the frequency shift for the adjacent resonating devices was 15X smaller for the in-plane micro-oven than for the in-cap micro-oven for the same amount of temperature increase for the ovenized elements. Similarly, the temperature increase was less than 3°C for the devices adjacent to the in-plane micro-oven. This is a very small effect in comparison to the almost 30°C raise in the devices adjacent to the in-cap micro-oven.

The IR images, shown in figure 5, captured while the in-plane ovenized DETF and the in-cap ovenized Lamé were ovenized show that the heat in the in-plane micro-oven is more uniformly distributed among the beams than the in-cap micro-oven. We approximate the temperature to be 215°C at the ovenized DETF, and 47.7 °C at the ovenized Lamé resonator based on the ratio of frequency shift to oven power. For the inplane oven, we were not able to discern any changes in temperature with the IR scope at a power lower than 60mW (ovenized element temperature of 180 °C), thus proving good thermal isolation.

The location of the adjacent devices with respect to the ovenized element seems to affect the frequency shift in the

devices, as shown by the plots in figure 7, which demonstrates that the closest device to the ovenized element is affected the most by the temperature change. In addition, differences in the ovenized elements could add to the frequency shift. A comparison of the same ovenized elements and with same layout could provide further insights into the effects due to placement of the devices and other possible sources of frequency drift.

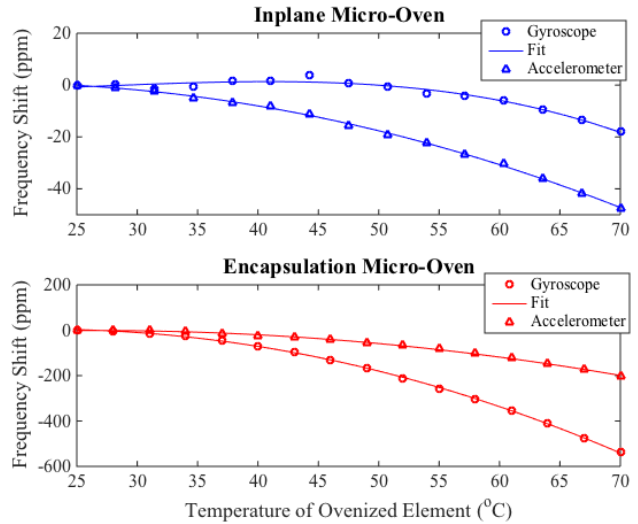


Figure 7: Frequency shift in each device with changes in micro-oven power required to heat element to 70°C.

### CONCLUSION

This work demonstrates that in-plane micro-oven can provide more than 10X reduction of heating of adjacent sensors when compared with in-cap layer micro-ovens. Thus, proving that in-plane ovenization temperature compensation techniques can significantly improve the overall operation of single-chip IMU/Clock systems with lower required power and fewer thermal effects on adjacent non-ovenized devices.

### ACKNOWLEDGEMENTS

This work was supported by the Defense Advanced Research Projects Agency (DARPA) Precision Navigation and Timing program (PNT) managed by Dr. Robert Lutwak under contract # N66001-12-1-4260. The fabrication work was performed at the Stanford Nanofabrication Facility (SNF) which was supported by National Science Foundation through the National Nanotechnology Infrastructure Network under Grant ECS-9731293. The author would also like to thank the National Science Foundation and the Graduate Research Program (NSF-GRFP) program.

### REFERENCES

- [1] Y. Chen, E. J. Ng, D. D. Shin, C. H. Ahn, Y. Yang, I. B. Flader, V. A. Hong, and T. W. Kenny, "Ovenized Dual-Mode Clock (ODMC) Based on Highly Doped Single Crystal Silicon Resonators", *Proc. 29<sup>th</sup> IEEE MEMS*, Shanghai, China, Jan. 24-28, 2016, pp. 91-94.
- [2] J. Salvia, R. Melamud, S. A. Chandorkar, S. F. Lord, and T. W. Kenny, "Real-Time Temperature

- Compensation of MEMS Oscillators Using an Integrated Micro-Oven and a Phase-Locked Loop”, *J. Microelectromech. Syst.*, Vol. 19, No. 1, pp. 192-2-1, 2010.
- [3] E. Ng, V. A. Hong, Y. Yang, C. H. Ahn, C. L. M. Everhart, and T. W. Kenny, “Temperature Dependence of the Elastic Constants of Doped Silicon”, *J. Microelectromech. Syst.*, Vol. 24, No. 3, pp. 730-741, 2015.
- [4] R. Melamud, S. A. Chandorkar, B. Kim, H. K. Lee, J. C. Salvia, G. Bahl, M. A. Hopcroft, and T. W. Kenny, “Temperature-Insensitive Composite Micromechanical Resonators”, *J. Microelectromech. Syst.*, Vol. 18, No. 6, pp. 1409-1419, 2009.
- [5] C. Jha, M. A. Hopcroft, S. A. Chandorkar, J. C. Salvia, M. Agarwal, R. N. Candler, R. Melamud, B. Kim, and T. W. Kenny, “Thermal Isolation of Encapsulated MEMS Resonators,” *J. Microelectromech. Syst.*, Vol. 17, No. 1, pp. 175-184, 2008.
- [6] A. Jaakkola, M. Prunnila, T. Pensala, J. Dekker, and P. Pekko, “Determination of doping and temperature-dependent elastic constants of degenerately doped silicon from MEMS resonators”, *IEEE UFFC*, Vol. 61, No. 7, pp. 1063-1074, 2014.
- [7] C. T.-C. Nguyen, and R. T. Howe, “Microresonator frequency control and stabilization using an integrated micro oven”, in *Digest Tech. Papers Transducers '93 Conference*, Yokohama, Japan, Jun. 7-10, 1993, pp. 1040-1043.
- [8] B. Kim, R. H. Olsson, and K. E. Wojciechowski, “Ovenized and thermally tunable aluminum nitride microresonators,” *IEEE Ultrason. Symp. (IUS)*, San Diego, CA, USA, Oct. 2010, pp. 974-978.
- [9] M. H. Li, C.-Y. Chen, C.-S. Li, C.-H. Chin, S.-S. Li, “A Monolithic CMOS-MEMS Oscillator Based on an Ultra-Low-Power Ovenized Micromechanical Resonator”, *J. Microelectromech. Syst.*, Vol. 24, No. 2, pp. 360-372, 2015.
- [10] J. Salvia, M. Messana, M. Ohline, M. A. Hopcroft, R. Melamud, S. A. Chandorkar, H. K. Lee, G. Bahl, B. Murmann, T. W. Kenny, “Exploring the Limits and Practicality of Q-based Temperature Compensation for Silicon Resonators,” *Proc. Electron Devices Meeting*, pp. 1-4, 2008.
- [11] B. Kim, R. N. Chandler, M. A. Hopcroft, M. Agarwal, W.-T. Park, and T. W. Kenny, “Frequency stability of wafer-scale film encapsulated silicon based MEMS resonators,” *Sens. Actuators, A*, Vol. 136, No. 1, pp. 125-131, 2007.
- [12] D. Yang, J.-K. Woo, S. Lee, J. Mitchell, A. D. Challoner, and K. Najafi, “A Micro Oven-Control System for Inertial Sensors”, *J. Microelectromech. Syst.*, Vol. 26, No. 3, pp. 507-518, 2017.
- [13] C.-Y. Liu, M.-H. Li, C.-Y. Chen, and S.-S. Li, “An Ovenized CMOS-MEMS Oscillator with Isothermal Resonator and Sub-mW Heating Power”, *IEEE IFCS*, New Orleans, LA, USA, May 9-12, 2016.
- [14] K. E. Wojciechowski, M. S. Baker, P. J. Clews, and R. H. Olsson, “A Fully Integrated Oven Controlled Microelectromechanical Oscillator Part I: Design and Fabrication,” *J. Microelectromech. Syst.*, Vol. 24, No. 6, pp. 1782-1794, 2015.
- [15] K. E. Wojciechowski, and R. H. Olsson, “A Fully Integrated Oven Controlled Microelectromechanical Oscillator Part II: Characterization and Measurement,” *J. Microelectromech. Syst.*, Vol. 24, No. 6, pp. 1795-1802, 2015.
- [16] J. Vig and Y. Kim, “The low-power potential of oven-controlled MEMS oscillators,” *IEEE Trans. Ultrason., Ferroelectr., Freq. Contr.*, Vol. 60, No. 4, pp. 851-853, Apr. 2013.
- [17] L. Christensen, C. H. Ahn, V. A. Hong, E. J. Ng, Y. Yang, B. J. Lee, and T. W. Kenny, “Hermetically encapsulated differential resonant accelerometer,” *IEEE 17th Int. Conf. on Solid-State Sensors*, Jun 2013, pp. 606-609.
- [18] C. H. Ahn, V. A. Hong, W. Park, Y. Yang, Y. Chen, E. J. Ng, J. Huynh, A. D. Challoner, K. E. Goodson, and T. W. Kenny, “On-chip ovenization of encapsulated Disk Resonator Gyroscope (drg)”, *IEEE 18th Int. Conf. on Solid-State Sensors*, Jun 2015, pp. 39-42.

## CONTACT

\*L. Comenencia Ortiz, tel: +1-787-608-9044;  
lcomenen@stanford.edu